

OLIN COLLEGE OF ENGINEERING

ENGR 3370: CONTROLS

---

# Guitar Tuner Final Report

---

*Authors:*

Jared KIRSCHNER

Molly FARISON

*Instructor:*

Dr. Kent LUNDBERG

May 7, 2012

## Introduction

In this project, we seek to build an automatic handheld guitar tuner so that amateur musicians can tune their instruments precisely and quickly. The tuner should sense the frequency of the current note and turn the tuning knob to tune each string with a single strum. We intend our first prototype to be a proof-of-concept model that tunes a single guitar note—the B string at 246.9 Hz.

Phase-locked loops (PLLs), widely used in radio and telecommunications applications, minimize phase error between two signals in order to lock the frequency of a voltage-controlled oscillator to a reference frequency. We implement our control system as a phase-locked loop with the guitar analogous to a voltage-controlled oscillator. This approach is used in order to create a fast analog control system, since a digital system based on acquiring the fundamental frequency through a digital FFT would not be fast enough to meet system requirements.

## 1 Design Requirements

The proof-of-concept prototype that tunes a specific guitar note with a single strum has design requirements in both usability and control. The mechanical, electrical, and compensator design must meet these requirements in order to be considered successful.

1. Settling time less than 5 seconds so that guitar can be tuned with a single strum
2. Zero steady-state error so that the note is precisely tuned
3. Ability to lock from 12.5 Hz of error, or a 90 degree turn of the tuning knob for our particular guitar
4. User can hold the tuner stationary on the tuning knob while strumming the guitar
5. Motor attached to coupling can turn the tuning knob given a constant input voltage

## 2 System Description and Model

A phase locked loop has three major components:

1. A phase detector which outputs a voltage proportional to a phase error
2. A loop filter which provides any necessary compensation
3. A voltage-controlled oscillator (VCO) which adjusts frequency from a zero-point with applied voltage

We chose to use an analog multiplier as the phase detector because the system signals are analog sinusoids. Given two input waveforms with angular frequencies  $\omega_1$  and  $\omega_2$  with amplitudes  $A_1$  and  $A_2$  respectively, the output of the analog multiplier is:

$$V_e = A_1 \cos(\omega_1 t) \times A_2 \cos(\omega_2 t + \phi) = \frac{A_1 A_2}{2} (\cos(|\omega_1 - \omega_2| + \phi) + \cos((\omega_1 + \omega_2) + \phi))$$

where  $\phi$  is the phase difference. After filtering out the high-frequency component, the equation becomes:

$$V_e = \frac{A_1 A_2}{2} \cos(|\omega_1 - \omega_2| + \phi) \quad (1)$$

If  $\omega_1 = \omega_2$ , we can see that the error is proportional to the product of the input sinusoid amplitudes  $A_1 A_2$ . In order for the control system to have a constant gain for a given error, the inputs  $A_1$  and  $A_2$  must be constant. The reference signal will have a constant amplitude, but the output of the guitar will not—it will decrease with time. We address this concern with an automatic gain control circuit, discussed in Section 4.

The guitar and tuning mechanism are analogous to the voltage-controlled oscillator. A guitar note is tuned by turning the associated tuning knob which determines the tension in the string. A DC brushed motor with a proper attachment on the shaft can be used to turn the tuning knob on the guitar in response to an input voltage. Together, the motor and the guitar constitute a VCO. To obtain a full model of the plant (VCO), we model the motor and the guitar separately.

First we consider the characteristics of the DC brushed motor. If we assume that the electrical time constant is significantly faster than the mechanical time constant and that there is zero damping, the motor can be modeled as:

$$\frac{\Theta_m}{V_m}(s) = \frac{1/k_t}{s(\tau s + 1)} \quad (2)$$

where  $\tau$  is the mechanical time constant,  $k_t$  is the motor transduction constant,  $\theta_m = \theta_k$  is the angle of the motor shaft coupled to the angle of the tuning knob, and  $V_m$  is the voltage applied to the motor. The components of the mechanical time constant are discussed further in Section 5. The effect of damping is not considered in our model due to the difficulties given available resources for characterizing that aspect of the motor.

Before performing an analysis on the guitar, we choose an appropriate reference. We treat the guitar string as a linear spring with a tension controlled by the angle of the tuning knob  $\theta_k$  passed through a gear system. The incremental change in frequency  $f_g$  is proportional to the square root of an incremental change in tension:

$$\Delta f_g = A\sqrt{(\Delta\theta_k)}$$

where  $A$  is a lumped constant of proportionality relating a change in tuning knob angle to a change in the fundamental frequency of the associated string. We linearize this model about our desired set point of 246.9 Hz to obtain an incremental, linear transfer function:

$$\frac{F_g}{\Theta_k}(s) = A$$

As the PLL will use the phase of the guitar output as the output signal, we obtain:

$$\frac{\Phi_g}{\Theta_k}(s) = \frac{A}{s} \quad (3)$$

If we linearize the phase detector as a multiplicative gain  $k_{pd}$ , the full uncompensated loop transfer function is:

$$\frac{\Phi_g}{V_m}(s) = k_{pd} \frac{1/k_t}{s(\tau s + 1)} \frac{A}{s} \quad (4)$$

A basic version of the full system model is shown in the following Simulink diagram:

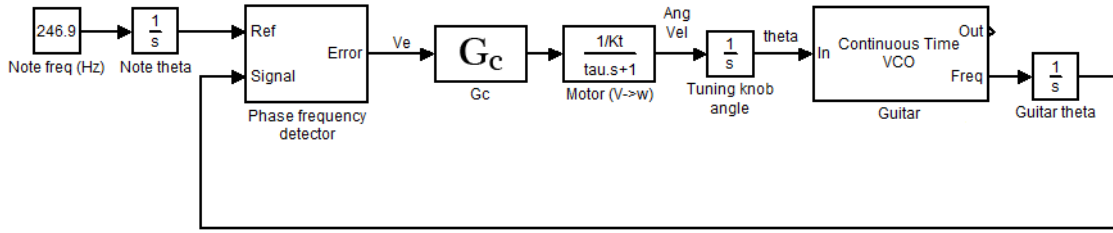


Figure 1: Full system model implemented as a phase-locked loop.

### 3 Hardware Design

#### 3.1 Mechanical Design

The mechanical system consists of:

1. A DC brushed motor
2. A small coupling that attaches to the motor shaft with a set screw on each side and interfaces with the guitar tuning knob
3. A box that stabilizes the motor, contains the electronics, and provides a way to hold the tuner easily.

Given that only small changes in angle are necessary to tune a guitar string and that turning the tuning knob requires a fair amount of torque, we selected a small motor with a gear ratio of 150:1 that is designed for high torque, low angular velocity applications. The coupling has been fully designed, tested, and machined. When affixed to the motor shaft, the motor could easily and reliably turn the guitar tuning knobs via the coupling. This system is shown in Figure 2. A plastic electronics box was selected to contain the motor and electronics, and attempts at using a metal box to reduce 60 Hz noise (discussed in Section 3.2) proved unsuccessful.

#### 3.2 Sensor

The sensor we are using is a piezoelectric acoustic guitar pickup—the Dean Markley Artist Transducer—which transduces the mechanical vibration of the guitar into an electrical signal. The sensor was clipped into a  $\frac{1}{4}$  inch jack. Leads were then soldered to the jack in order to provide a robust, low-noise interface between the sensor and the circuitry. This sensor produces a signal with an initial peak-to-peak amplitude of approximately 50 mV in response to strums. The result of the transduced signal passing through 10x amplification and a first-order bandpass filter with cut-offs of 222 Hz and 272 Hz can be seen in Figure 3. As shown in the image, the note’s harmonics are not fully attenuated even with a small-range bandpass filter. To investigate the harmonic spectrum, we recorded the sound made when strumming the B note of the guitar with a computer microphone and then performed an FFT. This analysis revealed that the third harmonic is particularly strong for this string and our strumming style. At certain tuning angles, the third harmonic was nearly as strong or stronger than the fundamental frequency. In addition to the unwanted harmonics, the signal contained approximately 5 mV of 60 Hz noise. Filter requirements and constraints are discussed in more depth in Section 6.2.

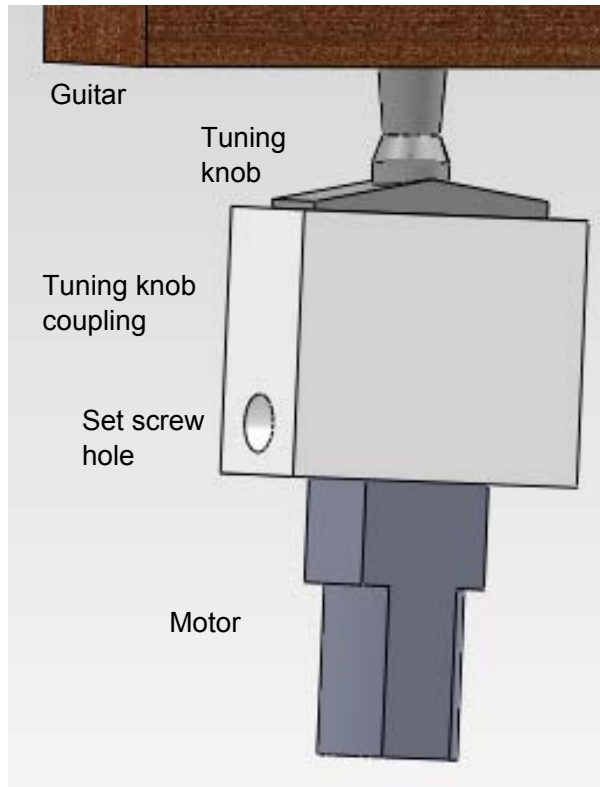
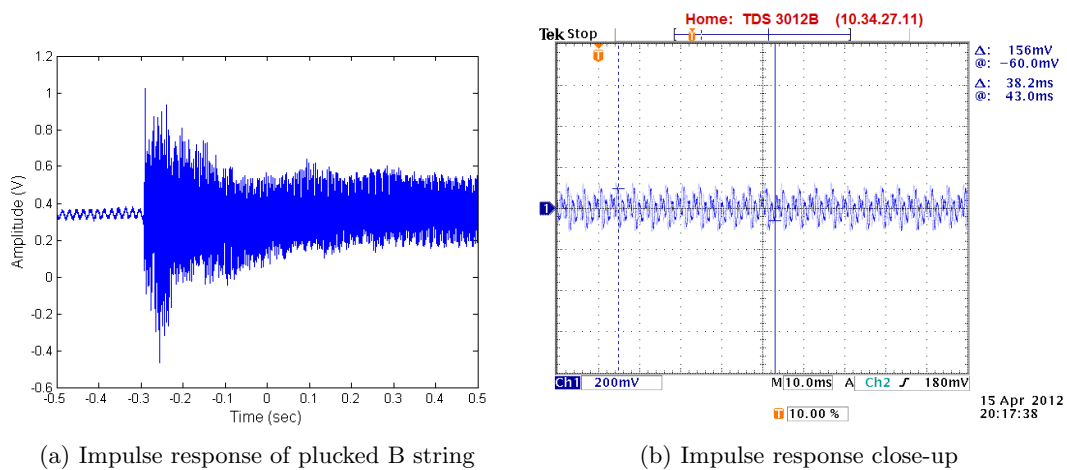


Figure 2: The motor shaft is attached by set screws to a coupling, which turns the guitar tuning knob.



(a) Impulse response of plucked B string

(b) Impulse response close-up

Figure 3: Filtered sensor data

## 4 Automatic Gain Control

Because the signal from the sensor fades as the sound from strumming the guitar fades, we used an automatic gain control (AGC) circuit to keep the sensor signal at an amplitude that is usable for phase detection in a phase-locked loop. We based our implementation on the circuit diagram shown in Figure 4.

This AGC circuit works as expected for an input signal from a function generator, as shown

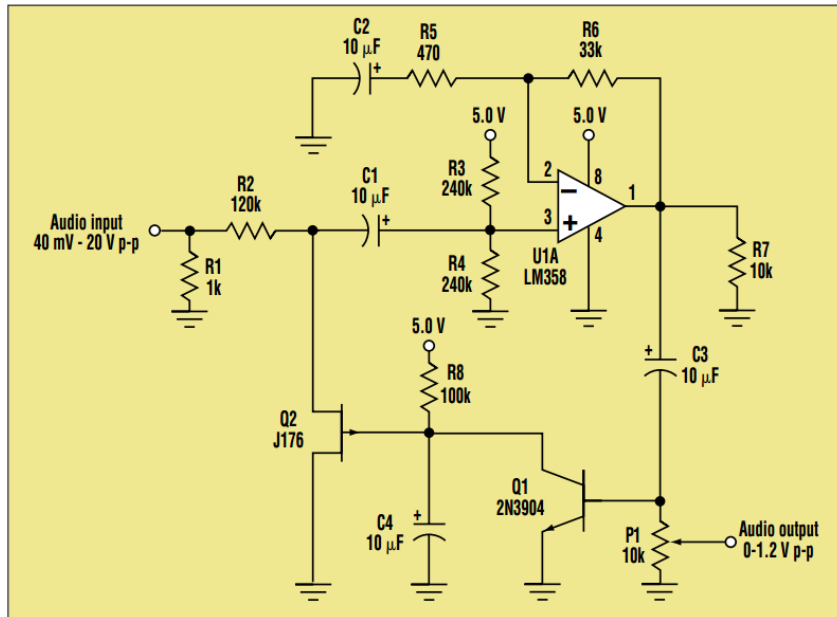
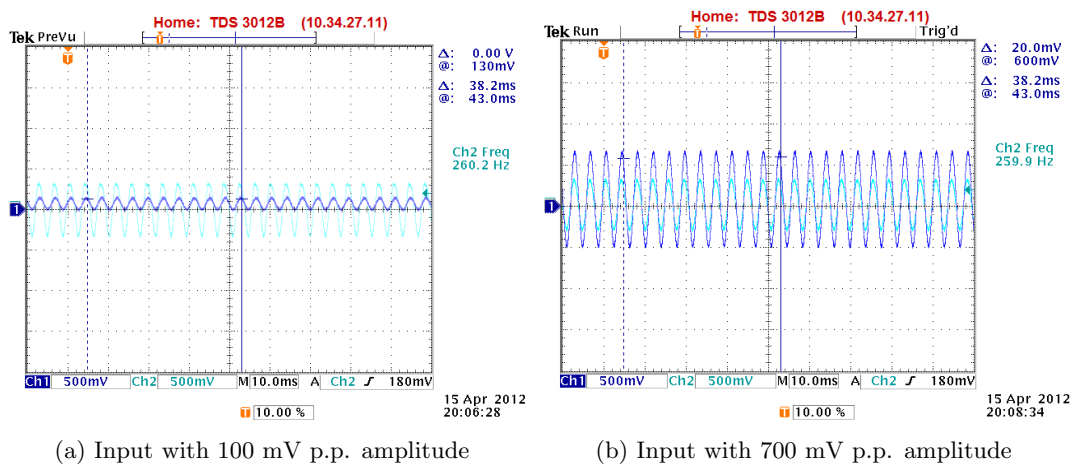


Figure 4: Basis for our automatic gain control circuit. Courtesy of George, Joseph P. *Effective AGC amplifier can be built at a nominal cost.* Electronic Design. August 3, 1998. Accessed at [http://www.bobblick.com/AGC\\_2IFD.pdf](http://www.bobblick.com/AGC_2IFD.pdf) on April 17, 2012.

in Figure 5. Channel 1 (dark blue) is the input function and channel 2 (cyan) is the output of the AGC circuit. Both graphs show the same output amplitude even though the first function input has a peak-to-peak amplitude of 100 mV and the second has an amplitude of 700 mV. We integrated the AGC with the output of the sensor to give it a constant amplitude for several seconds after each strum.



(a) Input with 100 mV p.p. amplitude

(b) Input with 700 mV p.p. amplitude

Figure 5: Demonstration of automatic gain control for two different input signal amplitudes. Input shown in dark blue; AGC output shown in cyan.

## 5 System Characterization

### 5.1 Guitar as a VCO

We modeled the guitar as a VCO with a transfer function of  $\frac{A}{s}$ .  $A$  describes the sensitivity of the note frequency to changes in the tuning knob angle. We found that  $A = \frac{25}{\pi}$  Hz/radian by measuring the frequency of the B string at various angles of the tuning knob and taking the mean of our measurements around the desired frequency of 246.9 Hz. These measurements were accomplished by recording the sound with a computer microphone and performing an FFT on the collected data.

### 5.2 Motor characterization

To parameterize the motor model shown in Equation 2, we must determine values for  $K_t$ ,  $R_m$ ,  $\tau$ , and  $J_m$ . The value of  $K_t$  was determined to be  $4.7 \times 10^{-2}$  Nm/A using the stall torque and stall current found on the motor's datasheet.  $R_m$  was determined to be 8.696  $\Omega$  by driving the motor with a slow square wave of voltage, then dividing  $\Delta v$  by  $\Delta i$ . The value of  $\tau$  was determined to be  $2.5 \times 10^{-2}$  s by measuring the settling time and using  $t_{s2\%} = 3.9\tau$ . The value of  $J_m$  was determined to be  $6.5 \times 10^{-6}$  Nms<sup>2</sup>/rad from the mechanical time constant relationship  $\tau = \frac{K_e K_t}{J_m R_m}$ . Note that  $K_e$  should be equal to  $K_t$ .

The motor also has a dead-zone nonlinearity that can be included in the model. The voltage applied to the motor in a given direction must be greater than approximately  $\pm 1$  V to cause motion.

The fully parameterized motor model is:

$$\frac{\Theta_m}{V_m}(s) = \frac{21.28}{s(0.02564s + 1)} \quad (5)$$

### 5.3 Additional considerations

The levels of 60 Hz noise and the 3rd harmonic of the vibrating string are particularly strong in the sensor output. These sources of noise must be accounted for in simulation. The AGC also contributes a phase shift between 30 and 40 degrees at the frequencies of interest in the system, greatly limiting the options for effective compensation.

### 5.4 Fully characterized system

The fully characterized system is shown in Figure 6. Substituting the system characteristics into Equation 4, we obtain:

$$\frac{\Phi_g}{V_m}(s) = \frac{169.3}{s^2(0.02564s + 1)}. \quad (6)$$

## 6 Compensation

### 6.1 Error signal phase margin

After many hours of exploration of the system behavior in simulation, we discovered a new stability requirement specific to phase-locked loops using an analog multiplier as the phase detector. In addition to the phase margin at crossover, the stability of a phase locked loop

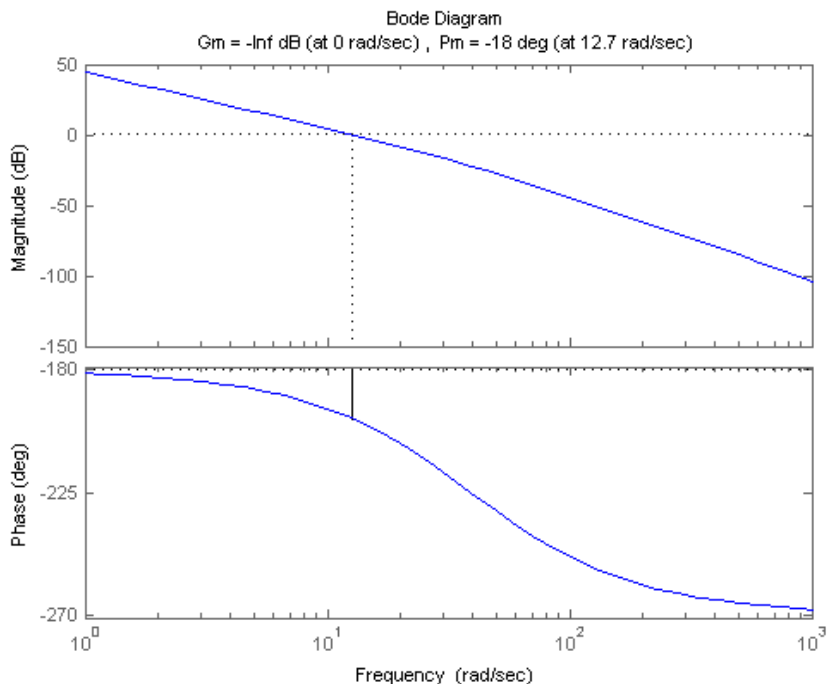


Figure 6: This Bode plot shows the loop transfer function of our uncompensated system as parameterized by the methods described in Section 5.

using an analog multiplier as the phase detector also depends on the phase margin at the frequency of the low-frequency error sinusoid.

Our intuition suggests that if the sinusoidal error signal is at least 180 degrees out of phase with the reference (input) signal, the motor will be driven in the opposite direction that it needs to be driven to obtain lock. Though this explanation is consistent with observation, it is not entirely convincing without a rigorous proof. Though we have not been able to work out a mathematical proof of this stability requirement, we present our case through simulation below in the following steps:

1. Construct the simplest PLL which can demonstrate the effect described
2. Add a low-pass filter to the output of the analog multiplier phase detector. Demonstrate that the behavior of the system remains essentially unaffected for initial error signal frequencies far from the phase crossover frequency
3. Demonstrate that as the initial error signal frequency approaches the phase crossover frequency, the stability of the system degrades. As the initial error frequency passes the phase crossover frequency, the system should become unstable
4. Add a lead compensator at the phase crossover frequency. Demonstrate that the system is now stable where it was not previously

The simplest possible PLL which can demonstrate this effect is a first-order PLL, with a slight modification. Let us assume a phase-locked loop with a loop gain of 25, a VCO of the form  $\frac{1}{s}$  and a quiescent frequency of 1000 rad/s, and a phase detector with output normalized so that the amplitude of each of its two frequency components is 1. Also assume a low-pass loop filter which significantly attenuates the high frequency component of the error signal but does

not affect the phase margin at crossover. This system has a crossover frequency of 25 rad/s and a phase margin of  $90^\circ$ . Unfortunately, its lock range is limited to  $\pm 25$  rad/s by its low frequency gain of 25, as shown in Figure 7. Because of this, the maximum frequency deviation our system can lock to is 25 rad/s, constraining the low-frequency component of the error signal below crossover. To demonstrate our effect, we must have the ability to lock onto frequencies with higher deviations than the crossover frequency of 25 rad/s. We increase the lock range of the system by adding a lag compensator with  $\alpha = 100$  and  $\tau = 10/25$  s. The final first-order PLL system diagram and loop transfer function are shown in Figure 8. The lock range has been significantly increased, as demonstrated by the step responses to 900 rad/s and 875 rad/s inputs in Figure 9.

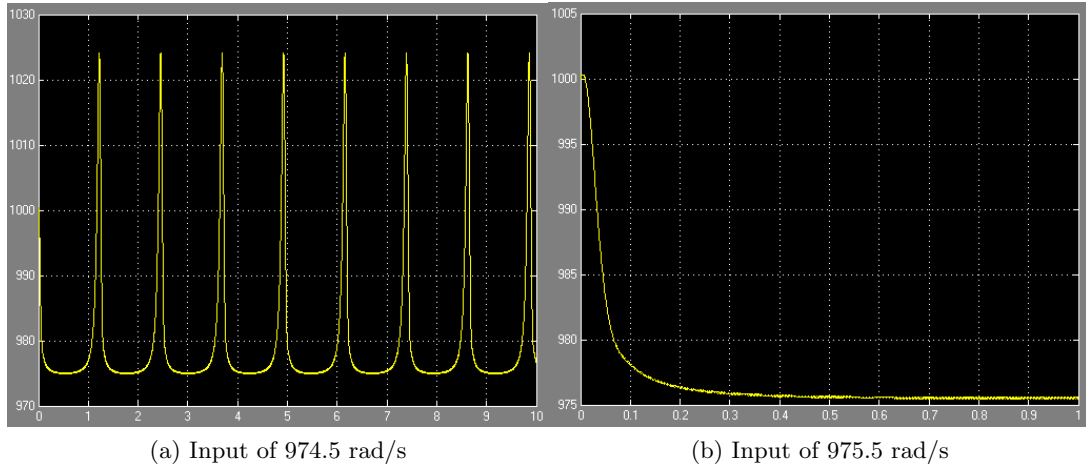
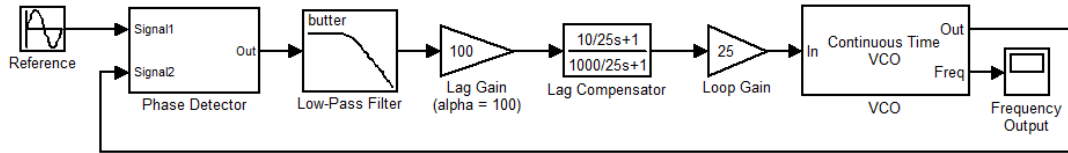


Figure 7: The lock range of the first-order PLL with a loop gain of 25 is limited to a 25 rad/s deviation from the quiescent frequency of 1000 rad/s. The system does not lock for an input of 974.5 rad/s (7a), but does for an input of 975.5 rad/s (7b). Note that this simulated system has a 4th-order low-pass Butterworth filter at 500 rad/s to get rid of the high frequency error signal noise. The cutoff frequency is high enough to leave the system unaffected at crossover.

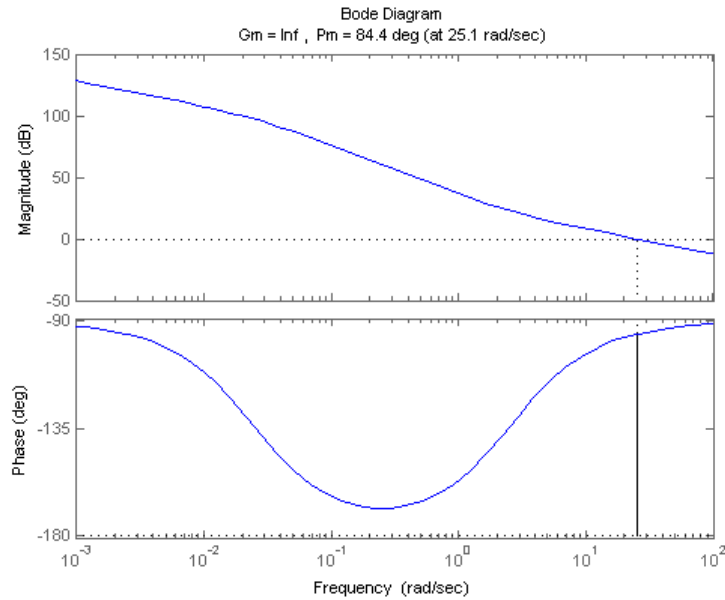
Now that we have demonstrated that the system can achieve lock to an input which produces an initial low-frequency error signal of 100 rad/s (and 125 rad/s), we will demonstrate the effect by forcing the phase crossover frequency of the system to be 100 rad/s. If our hypothesis is correct, the system should no longer be able to achieve lock to an input of 900 rad/s or less; in fact, the frequency of the system should move away from the set point over time. By making the loop filter a second-order, low-pass Butterworth filter with a cutoff frequency of 100 rad/s, we can add  $90^\circ$  of phase margin to our first-order system at 100 rad/s. This causes the phase crossover frequency to be 100 rad/s, as shown in Figure 10.

Figure 11 shows the step response of the system as the initial step increases past a deviation of 100 rad/s. It is clear that the system exhibits the behavior hypothesized as the initial low-frequency component of the error signal surpasses the phase crossover frequency.

Lastly, if the hypothesis is correct, we should be able to use lead compensation to increase the phase margin at the uncompensated phase crossover frequency. If we select a lead compensator with  $\alpha = 5$  centered at 100 rad/s, we obtain the compensated transfer function shown in Figure 12. This system has a phase crossover frequency of 168 rad/s, so we would expect the compensated system to be stable for input frequencies between 832 and 1068 rad/s. Figure 13 shows the step response of the system as the initial step responses increase past a deviation of 168 rad/s. We can see that while it is now stable past 100 rad/s, it is unstable past a deviation

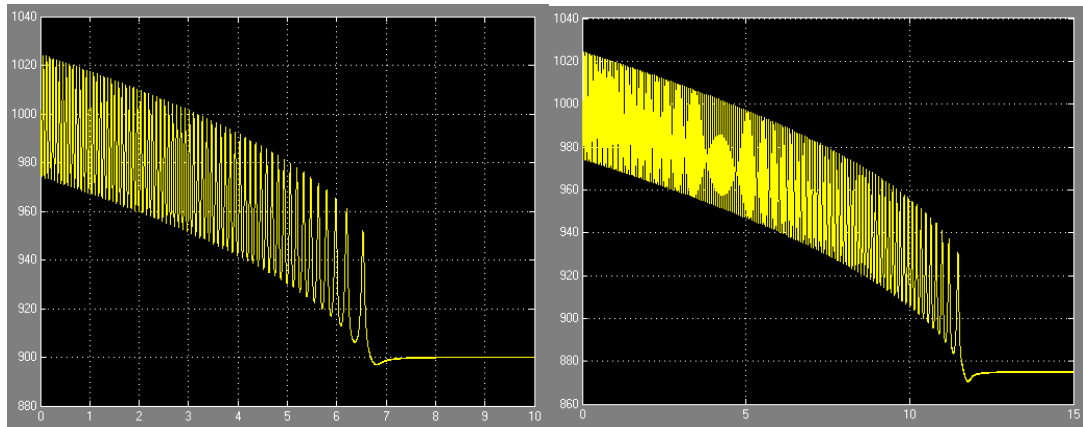


(a) System diagram



(b) Loop transfer function

Figure 8: First-order PLL with increased lock range.



(a) Input of 900 rad/s

(b) Input of 875 rad/s

Figure 9: First-order PLL with increased lock range. The system reaches lock for initial frequency deviations of 100 and 125 rad/s.

of 168 rad/s, as predicted.

This result indicates that the system must be compensated at both crossover and over our expected range of initial low-frequency error signals. In most systems with two poles at the

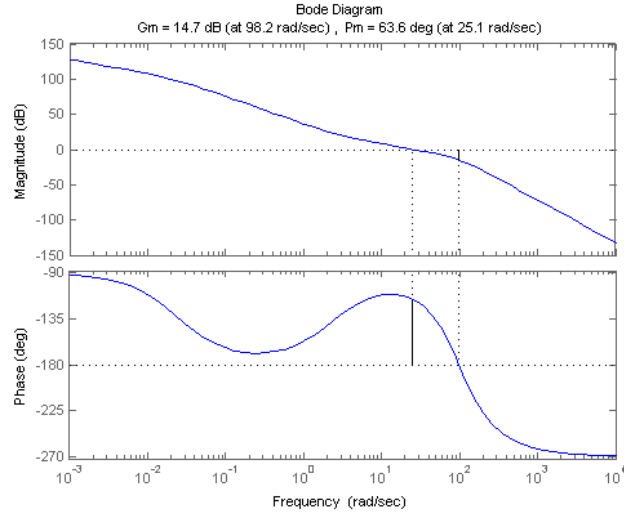


Figure 10: First-order PLL loop transfer function with a second-order, low-pass Butterworth filter with a cutoff frequency of 100 rad/s. Note that the phase crossover frequency has been made to be approximately 100 rad/s.

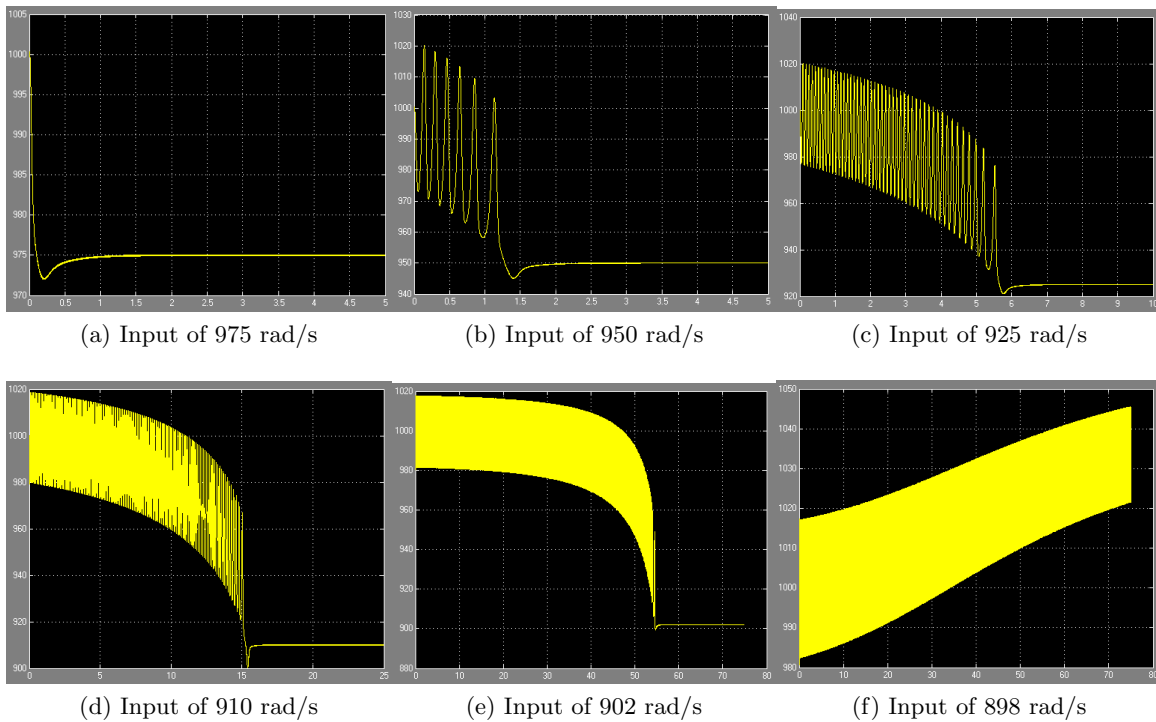


Figure 11: Step response of the system as the initial step increases past a frequency deviation of 100 rad/s. Note that as the initial low-frequency error signal approaches the phase crossover margin, the system takes an increasing amount of time to reach lock. As the frequency deviation passes 100 rad/s, the system is no longer stable, and moves away from the frequency setpoint forever.

origin and a third pole, the system can be made easier to compensate with lead by reducing the gain if the crossover is above the frequency of the third pole. This is not an option in our

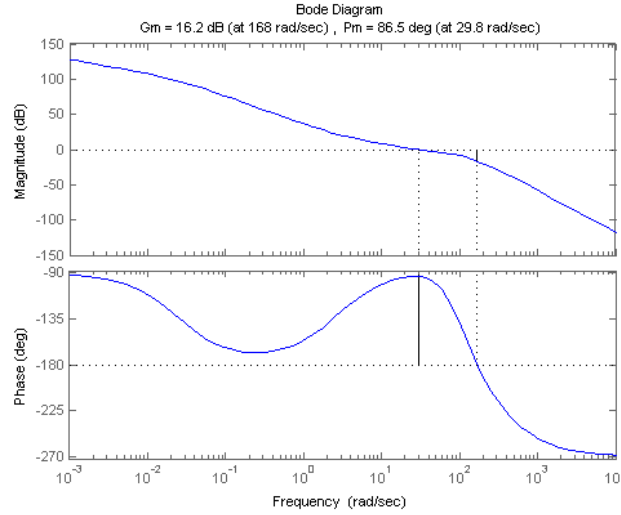


Figure 12: Compensated first-order PLL loop transfer function with a second-order, low-pass Butterworth filter with a cutoff frequency of 100 rad/s. Lead compensation has been used to increase phase margin at the phase crossover frequency ( $\approx 100$  rad/s).

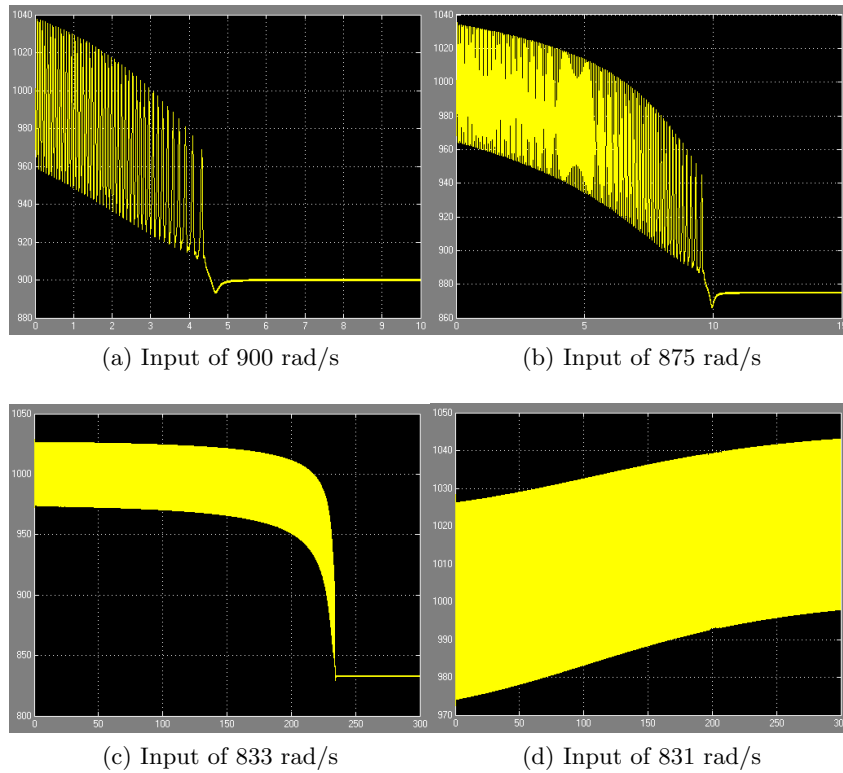


Figure 13: Step response of the system as the initial step increases past a frequency deviation of 168 rad/s. Note that as the initial low-frequency error signal approaches the phase crossover margin, the system takes an increasing amount of time to reach lock. As the frequency deviation passes 168 rad/s, the system is no longer stable, and moves away from the frequency setpoint forever. The system is now stable past 100 rad/s where the uncompensated system was not.

system, as the range of low-frequency error signals is determined by our system requirements.

## 6.2 Filtering

From the full system characterization described in Section 5, we determined the primary sources of noise within the system, as shown in Figure 14. For many systems, the noise requirement can be described as a level of noise rejection at specific high frequencies. As long as the loop transfer function has a low enough gain at the desired high frequencies, the requirements can be met. Unfortunately, this is not the case in our system for two reasons:

1. The frequencies of noise sources within our system are very close to the signal frequencies, making significant attenuation without a high-order filter difficult
2. Any attenuation near the expected range of error signal frequencies (0-15 Hz) will cause system instability, as discussed in Section 6.1

The frequencies of 60 Hz noise and the 3rd harmonics of desired note frequencies are very close to the error signal and fundamental frequencies that must be preserved for the system to be stable. The note B at 246.9 Hz, used as the tuning note for this prototype, is indicated on the number line. In order to effectively attenuate 60 Hz noise and 3rd harmonics while preserving the fundamental frequencies, especially for the lowest note E at 82.4 Hz, we would require a high-order bandpass filter. However, adding a high-order filter contributes an unwieldy amount of phase shift to the system at the frequencies of interest—the crossover frequency and the range of frequencies of the error signal. With no spare phase margin to sacrifice for a well-filtered output, we are left with a system that cannot both have useful filters and be stable. This also means that we will be unable to low-pass filter the output of the analog multiplier; the high-frequency component of the error signal is at  $\approx 2f_o$ , causing similar problems to those previously described.

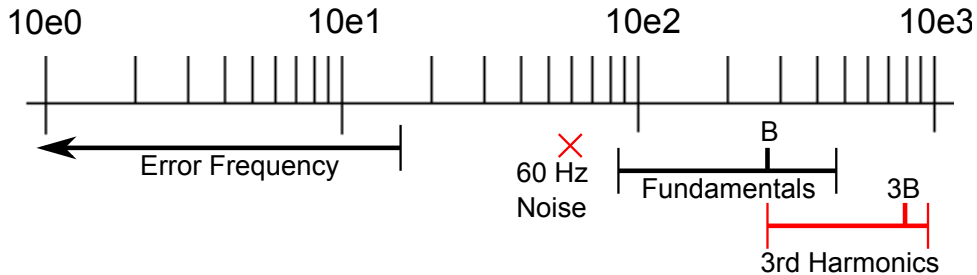


Figure 14: Frequencies of signals and noise sources in the system.

Because of our inability to filter the output of the guitar transduced by the piezoelectric pick-up, the analog multiplier will multiply each sinusoidal component of the output signal with the reference signal, resulting in a sum of sinusoids of the form shown in Equation 1. Even without a filter, the system will naturally respond more to the desired component of the error signal—a sinusoid with a frequency of the difference in frequencies between the reference and the fundamental frequency of the guitar string vibration. This raises the possibility that the system can still reach its frequency setpoint despite the large levels of noise; the remaining oscillations around the setpoint may be acceptable for the application. However, because we are unable to filter the output signal, there are two important considerations for system stability:

1. In a real system, the possibility of transient saturation is an important concern. As each noise sinusoid in the sensor output adds to the output of the analog multiplier, we must

be concerned about saturation from the output of the analog multiplier. The levels of noise in the sensor output limit the gain on the desired error signal which can be used without causing saturation.

2. Lead compensation increases the gain of the transfer function at high frequencies. The resulting increase in the amplitude of oscillations around the frequency setpoint may become unacceptable depending on the amount of lead compensation used.

### 6.3 Lead-Lag Compensation

As discussed at the end of Section 6.1, we will need lead compensation at both the crossover frequency and the upper range of the low-frequency error signals as determined by our requirements. As discussed in the beginning of Section 6.1, we should also use lag compensation to increase the lock range of our system. We found through simulation that a lag compensation  $\alpha$  of 10 was sufficient to increase the lock range of the system beyond our requirements ( $\pm 12.5$  Hz). If we place the voltage rails of our system at  $\pm 12$  V, we must choose the values of  $\alpha$  for both lead compensators carefully. At crossover, we only need a slight phase margin ( $\approx 30^\circ$ ). By increasing the  $\alpha$  of the lead compensator at crossover to the lowest possible value that meets our settling time requirements, we can increase the  $\alpha$  of the lead compensator for the low-frequency error signal, increasing the range of input frequency errors from which the system will have a stable response. Through some experimentation, we chose  $\alpha = 4$  for the lead compensator at crossover and  $\alpha = 6$  for the lead crossover for the low-frequency error signal. If we place the center of the crossover lead compensator at crossover, place the center of the error signal compensator such that this frequency becomes the compensated phase crossover frequency, and adjust the gain to place the maximum phase bump back at crossover, we obtain a system with a phase margin of  $35.2^\circ$  and a phase crossover frequency of  $67.3$  rad/s ( $\pm 10.7$  Hz). The final transfer function equation is shown in Equation 7, and its Bode plot is shown in Figure 15.

$$\frac{\Phi_g}{V_m}(s) = 4.24 \left( \frac{0.787s + 1}{7.87s + 1} \right) \left( \frac{0.157s + 1}{0.0394s + 1} \right) \left( \frac{0.0377s + 1}{0.00628s + 1} \right) \left( \frac{169.3}{s^2(0.02564s + 1)} \right) \quad (7)$$

We simulated the compensated system using the set-up shown in Figure 16. This simulation assumes a sensor signal with a constant amplitude of 500 mV, the output amplitude of our automatic gain control circuit. Based on the system characterization, we also model 60 Hz and third-harmonic noise signals of 125 mV. Simulation results for initial frequency errors increasing past the phase crossover frequency of 10.7 Hz are shown in Figure 17. The system meets specifications for initial frequency errors of less than 10.7 Hz. Note that the voltage signal going into the motor just barely avoids saturating on the  $\pm 12$  V rails, as shown in Figure 18. The continued oscillations even as the system approaches the setpoint are the result of the high-frequency component of the error signal which we cannot filter out, which also causes the low amplitude oscillations around the setpoint in the step responses shown in Figure 17.

Unfortunately, this system left out a critical factor that would have made compensation in the actual system not achievable. The automatic gain control circuit, which is critical for maintaining the output amplitude of the sensor signal from the guitar, has a phase-shift of  $30^\circ - 40^\circ$  for the frequencies of interest in the system. Given the other constraints of our system, we decided that a control system which satisfied our requirements could not be implemented.

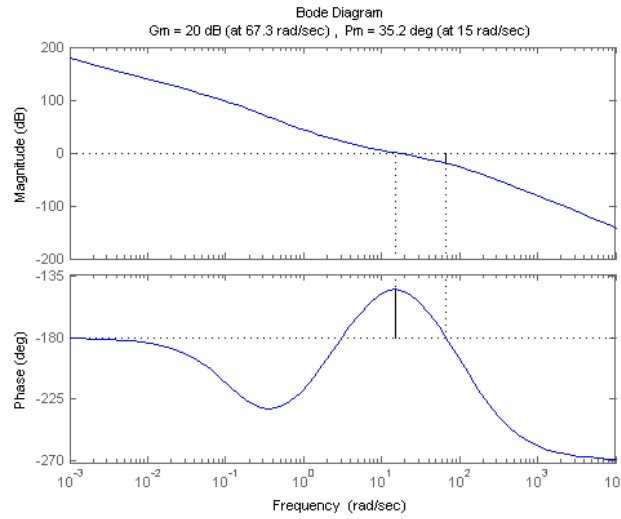


Figure 15: Bode plot of final compensated system, which uses two small lead compensators, a lag compensator, and an adjustable gain to maximize performance given the chosen design requirements and the system constraints.

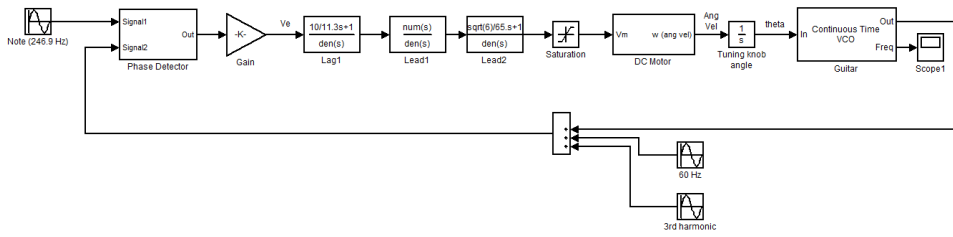


Figure 16: Model of final compensated system. Note: the automatic gain control circuit is implied in the model by the constant amplitude output of the VCO. The effects of the phase shift of the gain control circuit are not shown in this model, but are considered later in the analysis.

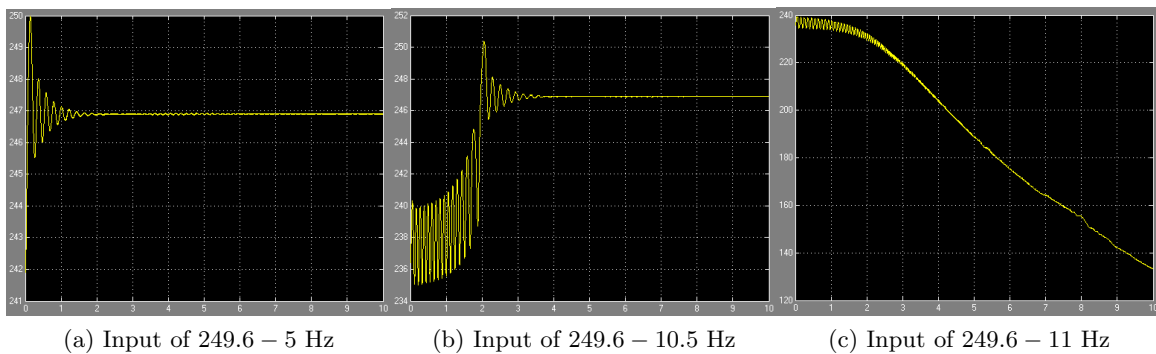


Figure 17: Simulation results for increasing initial frequency error inputs to the final compensated system. The system can achieve lock for initial frequency errors of less than 10.7 Hz.

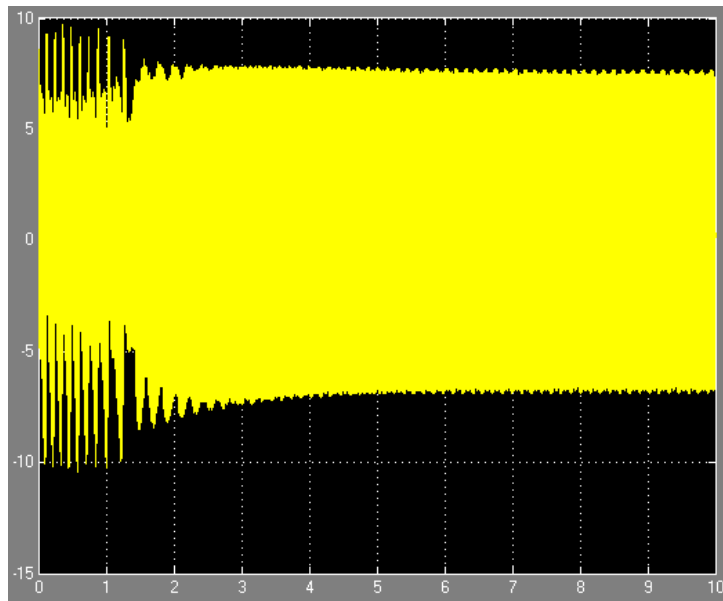


Figure 18: Voltage signal going into the motor. Note that the voltage signals approach the  $\pm 12$  V rails, leaving very little room to increase the  $\alpha$  values of the lead compensators. Large oscillations are present even when the system approaches lock due to the inability to filter the high-frequency component of the error signal from the analog multiplier.

## 7 Possibilities for System Improvement

One way to make system requirements achievable by decreasing phase shift would be to forgo the AGC and instead strum the guitar multiple times to tune. Though the control system would technically become unstable with decreased gain as the string vibration decays, this would manifest as a decreased control signal going to the motor, causing it to stop prematurely. With multiple strums, the control system might approach the setpoint. This system would be extremely inefficient because the signal amplitude decays rapidly, giving the system very little time to act during each strum.

Another way to expand possible solutions would be to use a motor with a faster time constant. The pole location of our motor is at 39 rad/s, contributing significant negative phase shift within the range of our low-frequency error signals, as shown in Figure 14. We are not sure whether faster motors with similar torque capabilities exist. The effective time constant of the motor could also be decreased through the use of minor loop compensation. Placing a proportional constant in a feedback loop around the motor would accomplish this. Unfortunately, minor loop compensation would cause transient saturation in our system. Because of the inability to filter out noise in the output signal that is fed into the analog multiplier, the signal going into the motor is pushed extremely close to the voltage rails, as discussed in Section 6.3. As minor loop compensation increases the initial amplitude of transient responses, even small gains would cause the system to saturate.